cells

MDPI

Article

Unlike Its Paralog LEDGF/p75, HRP-2 Is Dispensable for MLL-R Leukemogenesis but Important for Leukemic Cell Survival

Siska Van Belle [1,†], Sara El Ashkar [1,†], Kateřina Čermáková [2], Filip Matthijssens [3,4], Steven Goossens [4,5], Alessandro Canella [1], Courtney H. Hodges [6], Frauke Christ [1], Jan De Rijck [1], Pieter Van Vlierberghe [3,4], Václav Veverka [2,7] and Zeger Debyser [1,*]

1 Laboratory for Molecular Virology and Gene Therapy, Department of Pharmaceutical and Pharmacological Sciences, KU Leuven, 3000 Leuven, Belgium; siska.vanbelle@kuleuven.be (S.V.B.); sara.elashkar@gmail.com (S.E.A.); Alessandro.Canella@osumc.edu (A.C.); frauke.christ@kuleuven.be (F.C.); janderijck1@gmail.com (J.D.R.)
2 Institute of Organic Chemistry and Biochemistry, Academy of Sciences of the Czech Republic, Flemingovo nam. 2, 166 10 Prague, Czech Republic; Katerina.Cermakova@bcm.edu (K.Č.); vaclav.veverka@uochb.cas.cz (V.V.)
3 Department of Biomolecular Medicine, Ghent University, 9000 Ghent, Belgium; Filip.Matthijssens@UGent.be (F.M.); Pieter.VanVlierberghe@UGent.be (P.V.V.)
4 Cancer Research Institute Ghent (CRIG), 9000 Ghent, Belgium; Steven.Goossens@UGent.be
5 Department of Diagnostic Sciences, Ghent University, 9000 Ghent, Belgium
6 Department of Molecular & Cellular Biology, Center for Precision Environmental Health, and Dan L Duncan Comprehensive Cancer Center, Baylor College of Medicine, Houston, TX 77030, USA; Courtney.Hodges@bcm.edu
7 Department of Cell Biology, Faculty of Science, Charles University, 128 00 Prague, Czech Republic
* Correspondence: zeger.debyser@kuleuven.be; Tel.: +321-637-4029
† These authors contributed equally to the work.

Abstract: HDGF-related protein 2 (HRP-2) is a member of the Hepatoma-Derived Growth Factor-related protein family that harbors the structured PWWP and Integrase Binding Domain, known to associate with methylated histone tails or cellular and viral proteins, respectively. Interestingly, HRP-2 is a paralog of Lens Epithelium Derived Growth Factor p75 (LEDGF/p75), which is essential for *MLL*-rearranged (*MLL*-r) leukemia but dispensable for hematopoiesis. Sequel to these findings, we investigated the role of HRP-2 in hematopoiesis and *MLL*-r leukemia. Protein interactions were investigated by co-immunoprecipitation and validated using recombinant proteins in NMR. A systemic knockout mouse model was used to study normal hematopoiesis and MLL-ENL transformation upon the different HRP-2 genotypes. The role of HRP-2 in *MLL*-r and other leukemic, human cell lines was evaluated by lentiviral-mediated miRNA targeting HRP-2. We demonstrate that MLL and HRP-2 interact through a conserved interface, although this interaction proved less dependent on menin than the MLL-LEDGF/p75 interaction. The systemic HRP-2 knockout mice only revealed an increase in neutrophils in the peripheral blood, whereas the depletion of HRP-2 in leukemic cell lines and transformed primary murine cells resulted in reduced colony formation independently of *MLL*-rearrangements. In contrast, primary murine HRP-2 knockout cells were efficiently transformed by the MLL-ENL fusion, indicating that HRP-2, unlike LEDGF/p75, is dispensable for the transformation of MLL-ENL leukemogenesis but important for leukemic cell survival.

Keywords: leukemia; molecular cell biology; protein complex; protein-protein interaction; nuclear magnetic resonance (NMR); animal model; cell culture; hematopoietic stem cell; cell proliferation

check for updates

Citation: Van Belle, S.; El Ashkar, S.; Čermáková, K.; Matthijssens, F.; Goossens, S.; Canella, A.; Hodges, C.H.; Christ, F.; De Rijck, J.; Van Vlierberghe, P.; et al. Unlike Its Paralog LEDGF/p75, HRP-2 Is Dispensable for MLL-R Leukemogenesis but Important for Leukemic Cell Survival. *Cells* **2021**, *10*, 192. https://doi.org/10.3390/cells10010192

Received: 24 November 2020
Accepted: 15 January 2021
Published: 19 January 2021

1. Introduction

Mixed Lineage Leukemia (MLL)-rearranged leukemia is an aggressive, genetically distinct subset of acute leukemia. These rearrangements, involving the *11q23* locus, are

more frequently observed in infants, for which percentages range between 35% and 70% according to different studies [1–5]. Despite multiple efforts to develop a precision treatment, *MLL*-rearranged (*MLL*-r) acute leukemia remains associated with poor prognosis in children and adults, mostly due to tumor relapse, resulting in low 5-year survival rates [6]. The hallmark of this cancer is the translocation of the gene encoding MLL (*MLL1* or *KMT2A*) histone methyltransferase with one of more than 80 different partner genes, leading to the formation of oncogenic fusion proteins (MLL-FPs) [7]. The majority of MLL fusion partners are transcription regulators and promote the aberrant recruitment of the transcription machinery to the MLL target genes such as *HOX* genes (for review see Slany RK. [8]). To regulate gene expression, unstructured N-terminal motifs found in MLL form a ternary complex with menin and the integrase binding domain (IBD) of the p75 splice variant of Lens Epithelium Derived Growth Factor (LEDGF/p75). While LEDGF/p75 tethers the MLL-FPs to target genes, the sole molecular requirement for menin as an oncogenic cofactor in *MLL*-r leukemogenesis is to stabilize the interface of LEDGF/p75 with MLL-FPs [9]. Formation of the ternary complex is crucial for *MLL*-r leukemogenesis [9–11]. Importantly, LEDGF/p75 is dispensable for normal hematopoiesis, but required for the development of mixed lineage leukemia in mice [12].

HDGF, HDGF-related proteins 1 to 4 (HRP1-4) and LEDG, belong to the Hepatoma Derived Growth Factor (HDGF) family of proteins. The members are differentially expressed in both normal and pathological tissues, and their functions are not completely understood [13,14]. They are characterized by a high similarity in their N-terminal Homologue to Amino Terminus of HDGF (HATH) region [15]. This domain encompasses a PWWP-domain that specifically interacts with methylated lysines in histone tails [16]. Of note, HRP-2 and LEDGF/p75 are the only two members of this family harboring an IBD at their C-terminal end. LEDGF/p75 is a transcriptional co-activator that tethers IBD-binding proteins to the chromatin. Previous research indicated a role for LEDGF/p75 in DNA repair [17], cell survival and stress response [18–20], and various cancers [21–25].

The IBD domain of LEDGF/p75 is involved in the binding to the MLL-menin complex [9] and also known to interact with other cellular proteins including JPO2 [26], PogZ [27], ASK [28], IWS1 [29] and MED1 [30]. The affinity to the IBD domain is regulated by phosphorylation of the IBD binding motif (IBM) present on these binding partners [30]. In co-immunoprecipitation experiments PogZ, JPO2 and IWS1 were confirmed as HRP-2 binding partners [27,31].

In 2003, we reported that LEDGF/p75, next to cellular proteins, interacts with HIV integrase through the IBD [32,33]. By tethering the integration complex to the chromatin, LEDGF/p75 supports lentiviral integration and replication [32,34–36]. HRP-2 overexpression substitutes for the LEDGF/p75 function upon the depletion of the latter, presumably the consequence of the lower affinity of HIV-1 integrase for HRP-2 than for LEDGF/p75 [33,37]. Besides its role in HIV infection, HRP-2 has been linked to DNA repair by homologous recombination [38]. In addition, both HRP-2 and LEDGF/p75 were recently reported as key factors allowing RNA polymerase II to overcome the nucleosome-induced barrier to transcription elongation by taking over the FACT (facilitates chromatin transcription) complex role in differentiation to myotubes [39]. A myogenic function was also suggested by Zhang X. et al. [40]. HRP-2 is reported to be overexpressed in up to 40% of hepatocellular carcinoma cells where it promotes cancer cell growth in vitro as well as in vivo [31], whereas a reduction in HRP-2 was reported as a poor prognostic factor in Helicobacter pylori induced gastric cancer [41].

In light of this putative oncogenic activity, we compared HRP-2 with LEDGF/p75 in the context of hematopoiesis and *MLL*-r leukemia. Our data show that HRP-2 directly interacts with MLL in a menin-independent way. We report a systemic HRP-2 knockout mouse model with some postnatal mortality and modest changes in blood counts in the knockout survivors. In contrast to LEDGF/p75, HRP-2 appears to be dispensable for *MLL*-r leukemogenesis but required for leukemic cell survival.

2. Materials and Methods

2.1. Viral Vector Transductions and Generation of Stable Cell Lines

Viral vector productions were performed as previously described [12,42]. Titer units (TU) were determined by a p24 ELISA test (Fujirebio, Belgium). Human cell lines were transduced in a 1:1 volume ratio with concentrated lentiviral supernatants. Murine cells were transduced with pMSCV-based vectors as previously described [12]. Forty-eight hours post-transduction, cells were selected with puromycin at 1 µg/mL.

2.2. Protein Purification

All proteins were expressed in *E. coli* Rosetta2 (DE3), grown on Lysogeny Broth medium and supplemented with 10 mg/mL ampicillin. Flag-tagged LEDGF/p75 purification was performed as described before [43]. MBP-tagged HRP-$2_{470–552}$ and LEDGF/$p75_{325–530}$ were purified similarly as described for the latter in [44]. $MLL_{1–160}$-GST was purified as described in [45]. Expression and purification of LEDGF/$p75_{345–426}$ was described earlier [46]. Identical conditions were used for expression and purification of HRP-$2_{469–549}$. Protein fractions were analyzed by SDS-PAGE and Coomassie stain. Peak fractions were pooled.

2.3. AlphaScreen Assay

The AlphaScreen assay was performed as described before [30]. Flag-LEDGF/p75 (0.3 nM) was preincubated with $MLL_{1–160}$–GST (10 nM) before titration of MBP-LEDGF/$p75_{325–530}$, MBP-HRP-$2_{470–552}$ or MBP alone at the indicated concentrations.

2.4. Co-Immunoprecipitation (IP)

Six million HEK293T cells were plated in a 8.5 cm petri dish and transfected with 20 µg of each indicated plasmid (three petri dishes/condition) and lysed as described in [30]. For IP experiments with MI-2 and MI-538 (MedChem Express), respectively 100 µM and 50 µM of the compound (or DMSO control) was added during lysis and overnight incubation. Immunoprecipitated protein was eluted with SDS-PAGE loading buffer and visualized by western blotting.

2.5. Peptide Synthesis

The peptides used in this study were synthesized by solid-phase synthesis in the Laboratory of Medicinal chemistry, IOCB, ASCR (Prague, Czech Republic).

2.6. NMR Spectroscopy

NMR spectra were acquired at 25 °C on the 850 MHz Bruker Avance spectrometer equipped with a triple-resonance ($^{15}N/^{13}C/^{1}H$) cryoprobe. For structure determination, the sample volume was 0.35 mL, with a concentration of 500 µM HRP-$2_{469–549}$ in the NMR buffer (25 mM TRIS pH 7.0, 150 mM NaCl, 1 mM TCEP), 5% D_2O/95% H_2O. The sequence-specific backbone and side-chain resonance assignment were obtained using a series of standard triple-resonance spectra (HNCO, HN(CA)CO, HNCACB, CBCA(CO)NH, HBHA(CO)NH, CCC(CO)HN and HCCH-TOCSY [47,48]). ^{1}H-^{1}H distance constraints for structural determination were obtained from intensities of NOE cross peaks in the 3D $^{15}N/^{1}H$ NOESY-HSQC and $^{13}C/^{1}H$ NOESY-HMQC spectra that were acquired using a NOE mixing time of 100 ms.

The families of converged structures were initially calculated in Cyana 3.98 using the combined automated NOE assignment and structure determination protocol [49]. In addition, backbone torsion angle constraints, generated from assigned chemical shifts using the program TALOS+ [50] were included in the calculations. Subsequently, five cycles of simulated annealing combined with redundant dihedral angle constraints were used to produce sets of converged structures with no significant restraint violations (distance and van der Waals violations < 0.2 Å and dihedral angle constraint violation < 5°), which were further refined in explicit solvent using the YASARA software with the YASARA forcefield [51]. The 30 HRP-2 IBD structures with the lowest total energy were selected,

analyzed and validated using the Protein Structure Validation Software suite (http://psvs-1_5-dev.nesg.org). The constraints and structural quality statistics for the final set of water-refined HRP-2 IBD structures is summarized in Supplementary Table S1. The structure, NMR constraints, and resonance assignments were deposited in the Protein Data Bank (PDB, accession number 6T3I) and Biological Magnetic Resonance Bank (BMRB, accession number 34442).

In titration experiments 20 µM of ^{15}N-labeled HRP-$2_{469–549}$ or LEDGF/$p75_{345–426}$ were mixed with various concentrations of unlabeled synthetic MLL peptide (123–160) or DMSO as a control. For each titration point, the chemical shift perturbations (CSP) in ^{15}N/^{1}H HSQC spectra measured in the SOFAST fashion were calculated and the dissociation constant was determined by a non-linear least squares analysis using GraphPad Prism and the equation

$$CSP_{obs} = CSP_{max} \times \frac{[L] + [P] + K_D - \sqrt{([L] + [P] + K_D)^2 - 4 \times [L] \times [P]}}{2 \times [P]}$$

where CSP_{obs} is the observed CSP at the given total ligand concentration [L], CSP_{max} is the CSP at saturation, and [P] is the total concentration of protein [52].

2.7. HRP-2 Knockout Mouse Mode

C57BL/6N-Hdgfrp2<tm1b (KOMP)Wtsi>/Tcp (*HRP-2*^{tm1b}) mice were ordered at Toronto Centre for Penogenomics after they were generated as part of the NorCOMM2 phenotyping project [53]. All animal experiments were approved by the KU Leuven ethical committee (P201/2014).

2.8. Clonogenic Growth In Vitro

Primary murine lin$^-$ cells were cultured and scored in a semisolid colony formation unit (CFU) assay as described before [12]. Human, immortalized cell lines were cultured in MethoCult^{TM} H4230 (STEMCELL Technologies) and scored after 10 days in culture.

2.9. RNA-Sequencing and Bioinformatics

Total RNA samples (500 ng) were cleaned using the DNAse I kit (Thermoscientific) according to the Rapid out removal DNA kit instruction and converted into cDNA by using the QuantSeq 3′ mRNA-seq reverse 4 Library Prep Kit (Lexogen) according to manufacturer's instructions [54] to generate a compatible library for Illumina sequencing. Briefly, library generation was initiated by oligodT priming for first strand cDNA which generated one fragment per transcript. The second strand cDNA was subsequently synthesized using random primers. Illumina-specific linker sequences were introduced by the primer with barcoding indices for different samples. The quality of cDNA libraries was determined using a High Sensitivity DNA Assay 2100 Bioanalyzer (Agilent) for quality control analysis. Sequencing of the cDNA library with 75bp single end reads was performed using an Illumina NextSeq 500 system. Reads were aligned to the reference genome GRCm38 using STAR-2.4.2a with default settings [55]. STAR was also used for gene expression quantification on the Ensembl GTF file version 84. Differential expression analysis was performed using DESeq2 in R [56]. The RNA-sequencing data are available in NCBI's Gene Expression Omnibus (GSE154202).

2.10. Statistical Analysis

The presented graphs were generated using GraphPad Prism 8.3.1. The experimental results from in vitro experiments are presented as means ± standard deviations. Sample sizes (n) and description of each experimental group or condition are indicated in the figure legends. Different groups were statistically evaluated by a two-sided student's t-test (for $n > 4$) or Mann–Whitney U test (for $n = 4$) using GraphPad Prism 8.3.1 and p-values below 0.05 were considered significantly different.

3. Results

3.1. HRP-2 Interacts with MLL in the Absence of Menin

HRP-2 and LEDGF/p75 are the only two human proteins that contain both the PWWP and the IBD domains (Figure 1A) [15,33]. As both HRP-2 and LEDGF/p75 can fulfil a similar role in HIV infection [33,37] and LEDGF/p75 is important for *MLL*-r [9,12], we investigated the involvement of HRP-2 in hematopoiesis and MLL-mediated transformation. Menin serves as an adaptor to link MLL with LEDGF/p75 and thus is essential for the formation of the triple transcription-regulatory complex [9]. Here, we investigated the potential interaction of HRP-2 with the MLL-menin complex by in vitro co-immunoprecipitation (IP) in HEK293T cells transfected with flag-tagged MLL-ELL and/or menin-HA expression constructs (Figure 1B–E). The binding of endogenous HRP-2 and LEDGF/p75 was detected using anti-HRP-2 or anti-LEDGF antibodies. Despite the poor detection of flag-MLL-ELL in the precipitate in the absence of ectopic menin expression, it is clear that upon the overexpression of menin and MLL, both HRP-2 and LEDGF/p75 were precipitated. To further clarify whether the binding of HRP-2 to MLL-ELL is dependent on menin, as is the case for LEDGF/p75, we treated cellular lysates with 100 μM of MI-2 [57], a previously described MLL-menin interaction inhibitor. In line with previous reports, MI-2 treatment resulted in a partial loss of menin binding upon MLL precipitation (Figure 1C) [57]. HRP-2 still co-precipitated with MLL upon MI-2 treatment. Similar results were obtained using 50 μM of the more potent MI-538 inhibitor (Figure 1D) [58]. Since both menin inhibitors did not fully abrogate the MLL-menin interaction, we introduced three point mutations (F9A, P10A and P13A) into a flag-MLL-$ELL_{1–330}$ (MLL Mut), known to completely abolish binding to menin [59]. Whereas the MLL mutations did not interfere with the precipitation of HRP-2 (Figure 1E), the MLL mutant failed to co-IP LEDGF/p75 despite the presence of overexpressed menin, suggesting HRP-2 is less dependent on menin for binding to MLL. Interestingly, whereas ectopic overexpression of menin resulted in increased co-precipitation of LEDGF/p75, binding to HRP-2 was reduced, supporting a competition between HRP-2 and LEDGF/p75 for binding to MLL under control of menin (Figure 1B,E).

3.2. HRP-2 and LEDGF/p75 Interact with MLL through a Conserved Interface with Similar Affinities

To obtain a detailed insight into the mechanism of the MLL and HRP-2 association, we determined the solution structure of the HRP-2-IBD domain (amino acids 469–549, Figure 2A). The solution structure of the HRP-2-IBD revealed a compact right-handed bundle composed of five α-helices, comparable to other members of the TFIIS N-terminal domain family and demonstrated a high degree of structural conservation between LEDGF/p75 and HRP-2 IBDs (Figure 2C).

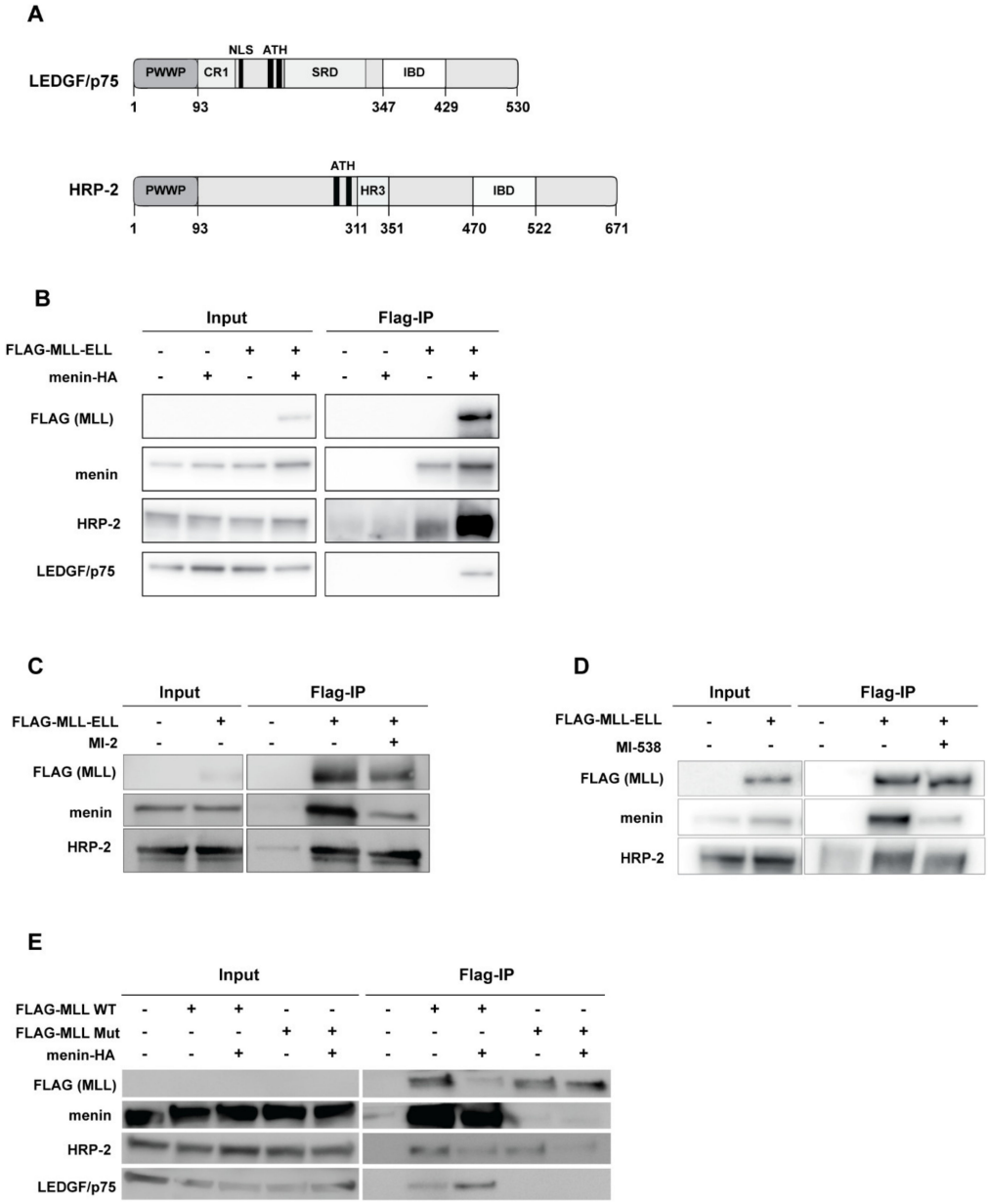

Figure 1. Menin is dispensable for the interaction of MLL and HRP-2. (**A**) Schematic representation of the domain structure of LEDGF/p75 and HRP-2. The N-terminus of LEDGF comprises the PWWP domain, the nuclear localization signal (NLS), AT hooks (ATH) and four charged regions (CR), of which CR2-4 contain a supercoiled DNA recognition domain (SRD). At the C-terminus, LEDGF/p75 harbors the integrase binding domain (IBD) [60]. HRP-2 harbors an N-terminal PWWP domain, two AT hooks, a patch of conserved amino acids known as homology region III (HR3) and a C-terminal IBD domain; (**B**) HEK293T cells were transfected with flag-tagged MLL-ELL and/or menin-HA expression constructs as indicated. Flag-MLL-ELL was immunoprecipitated using anti-flag beads and analyzed using antibodies against flag. Menin, endogenous HRP-2 and LEDGF/p75 were detected using specific antibodies; (**C**,**D**) HEK293T cells were transfected with flag-tagged MLL-ELL as indicated. MLL-ELL was immunoprecipitated using anti-flag beads in the presence of a previously described menin-MLL interaction inhibitor (**C**) MI-2 [57] or (**D**) more potent MI-538 [58], at concentrations of 100 and 50 μM respectively or DMSO control. Precipitated proteins were analyzed by western blot. Flag antibodies were used for the detection of MLL-ELL. Endogenous levels of menin, HRP-2 and LEDGF/p75 were detected using specific antibodies; (**E**) HEK293T cells were transfected with flag-tagged wild-type MLL-ELL$_{1–330}$ (MLL WT) or a menin interaction-deficient construct 'MLL Mut' with point mutations F9A, P10A and P13A and/or menin-HA as indicated. Due to low expression levels, MLL$_{1-330}$ is not detected in the input by flag antibody. Endogenous levels of menin, LEDGF/p75 and HRP-2 are detected using specific antibodies. Details about the western blot analysis can be found in supplementary information.

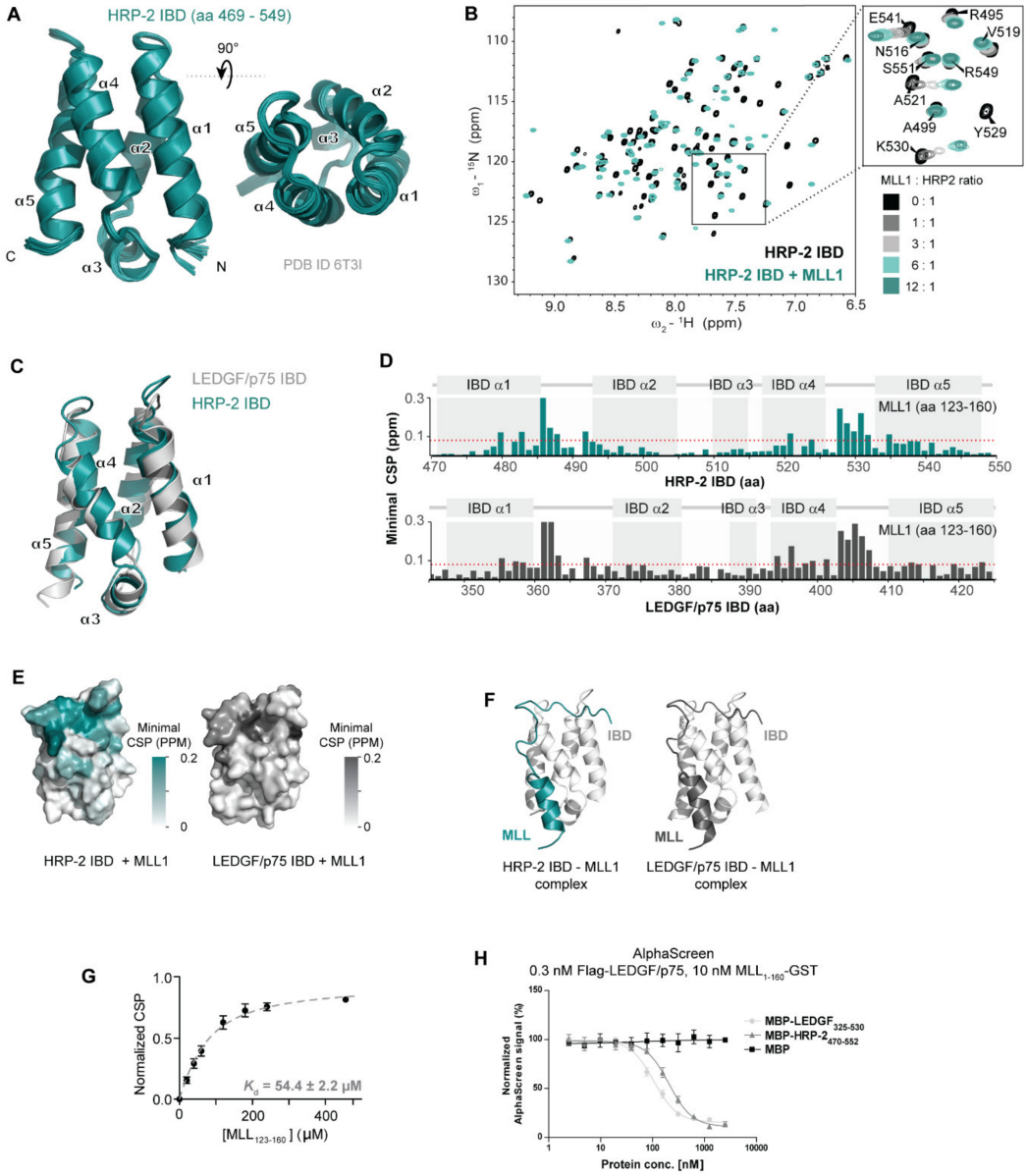

Figure 2. HRP-2 IBD and LEDGF/p75 IBD interact with MLL in a conserved manner. (**A**) Solution structure of HRP-2 IBD (PDB ID 6T3I); (**B**) HRP-2-IBD directly interacts with the identical consensus motif of MLL (amino acids 123-160) alike LEDGF/p75-IBD as determined by NMR spectroscopy. Comparison of the $15^N/1^H$ HSQC spectra of the 20 µM HRP-2 IBD in the absence (black) and presence (green) of 120 µM $MLL_{123–160}$. On the right, detail HRP-2 IBD titration with $MLL_{123–160}$. HSQC spectra are colored based on $MLL_{123–160}$ concentration as indicated in the figure. The spectra were obtained from the 15^N-labeled recombinant IBD and the unlabeled synthetic MLL-derived peptide; (**C**) Superposition of HRP-2-IBD (green) and LEDGF/p75-IBD (light grey) solution structures; (**D**,**E**) Comparison of the HRP-2-IBD–$MLL_{123–160}$ and LEDGF/p75-IBD –$MLL_{123–160}$ interaction surfaces. Representation of the minimal chemical shift perturbation (CSP) in backbone amide signals of the IBDs upon addition of $MLL_{123–160}$ peptide in panel D. Amino acid residues that are significantly perturbed upon addition of $MLL_{123–160}$ to HRP-2-IBD or LEDGF/p75-IBD (as determined by NMR spectroscopy) are highlighted in green or gray on the surface of the IBD structures in panel E; (**F**) Comparison of homology model of MLL-HRP-2-IBD and solution structure of MLL-LEDGF/p75-IBD solution structure (PDB ID 6emq); (**G**) K_d fit from NMR titrations of HRP-2-IBD with $MLL_{123–160}$. Dissociation constant was determined by following the chemical shift perturbations of the HRP-2-IBD backbone amide signals induced upon titration with $MLL_{123–160}$. Error bars represent the error of the fit for most perturbed residues (n = 10); (**H**) Alpha Screen. Full length flag-tagged LEDGF/p75 (0.3 nM) was incubated with GST-tagged $MLL_{1–160}$ (10 nM) in an out competition Alpha Screen assay. C-terminal fragments of LEDGF/p75 ($LEDGF_{325–530}$) and HRP-2 ($HRP\text{-}2_{470–552}$) were titrated to outcompete the interaction.

To validate and characterize the direct interaction between HRP-2-IBD and MLL, we followed the changes in positions of backbone NMR signals of ^{15}N-labeled HRP-2-IBD either in absence or presence of different concentrations of a synthetic MLL-derived peptide (amino acids 123-160). $MLL_{123–160}$ induced significant chemical shift perturbations of the IBD backbone signals (Figure 2B and Figure S1). Moreover, this experiment revealed that MLL recognizes HRP-2-IBD through the same interface and binds with similar affinity as LEDGF/p75 (Figure 2D–H). In particular, the chemical shift perturbations in the IBD backbone induced by binding of $MLL_{123–160}$ were found in two regions (amino acids 479–492 and 520–535) (Figure 2D). As for the LEDGF/p75 IBD-$MLL_{123–160}$ interaction [46], these regions form two interhelical loops connecting IBD α helices α1–α2 and α4–α5, respectively (Figure 2E,F). Additionally, the analysis of the chemical shift perturbations in the HRP-2 IBD backbone induced by binding of JPO2 (amino acids 1–130) and POGZ (amino acids 1117–1410) revealed a pattern remarkably similar to that induced upon addition of MLL confirming that these protein fragments bind to HRP-2 in the same conserved structural mode as LEDGF/p75 IBD (Figure S2). Importantly, the dissociation constants for the $MLL_{123–160}$ interaction with HRP-2-IBD (54.4 ± 2.2 μM, Figure 2G) obtained from NMR titration experiments are comparable with those of LEDGF/p75 (64.0 ± 6.5 μM) obtained in our earlier studies [30]. In addition, HRP-2 and LEDGF/p75 affinities to MLL were compared in an AlphaScreen assay with MBP-fused recombinant C-terminal fragments of LEDGF/p75 ($LEDGF_{325–530}$) and HRP-2 ($HRP\text{-}2_{470–552}$), purified from E. *coli* and used to outcompete the interaction between recombinant flag-tagged LEDGF/p75 and GST-tagged N-terminal fragment of MLL ($MLL_{1–160}$–GST). Unlike MBP alone, both IBD domains of HRP-2 and LEDGF/p75 efficiently outcompeted the interaction between $MLL_{1–160}$–GST and full-length flag-LEDGF/p75 (Figure 2H). Altogether, our data revealed that the overall binding mechanism used by HRP-2 and LEDGF/p75 IBDs is highly conserved.

3.3. Systemic HRP-2 Depletion in Mice Leads to Increased Postnatal Mortality and Decreased In Vitro Colony Formation of Hematopoietic Stem Cells

To better understand the importance of the MLL-HRP-2 interaction, we investigated a systemic knockout mouse model (from the Toronto Centre Phenogenomic, Toronto, ON, Canada) to address the role of HRP-2 in postnatal hematopoiesis. The depletion of HRP-2 mRNA and protein levels in these knockout (*HRP-2*$^{-/-}$) mice were confirmed by quantitative PCR (qPCR) and Western blot in bone marrow cells (Figure S3A). With percentages of 61% and 29.5%, observation of inbred crossings revealed increased numbers of heterozygous (*HRP-2*$^{+/-}$) and wild type (*HRP-2*$^{+/+}$) mice, respectively, at age of 6 to 8 weeks in regard to the expected Mendelian inheritance pattern (Table 1). Moreover, *HRP-2*$^{-/-}$ mice were present at a lower percentage (9.5%) than expected. At one day after birth, the ratio of *HRP-2*$^{-/-}$ mice corresponded more closely to the expected Mendelian ratio by representing 20% of newborn pups.

Table 1. Genotype of heterozygous (*HRP-2*$^{+/-}$) crossed offspring after birth or weaning (6 to 8 weeks).

Age	Number (%) of Mice		
	***HRP-2*$^{+/+}$**	***HRP-2*$^{+/-}$**	***HRP-2*$^{-/-}$**
1 day	36 (23.2)	88 (56.7)	31 (20.0)
6–8 weeks	31 (29.5)	64 (61.0)	10 (9.5)
Expected values	25%	50%	25%

In contrast to an earlier report by Wang et al. [61], we observed that *HRP-2*$^{-/-}$ pups presented with increased mortality before 6–8 weeks of age, suggesting that HRP-2 is important for postnatal survival early after birth. Read-through of the gene trap could explain discrepancies between both models, since Wang et al. showed a 5–20% residual *HRP-2* expression in their model, while *HRP-2* mRNA levels in hematopoietic stem cells (HSC) of our few surviving mice were undetectable by qPCR (Figure S3A).

To compare steady-state hematopoiesis between weaned wild type and knockout mice, blood counts were analyzed for the different genotypes. No significant differences were observed in total white and red blood cell count (Figure 3A top), whereas the differential blood count revealed a significant increase in neutrophils in the *HRP-2*$^{-/-}$ mice compared to the wild type (p = 0.042, Figure 3A bottom). Other cell types did not differ between genotypes (Figure S3B). To explore the functionality of the cells, we sought to compare the colony-forming capacity of *HRP-2* wild type, heterozygous and knockout cells using myeloid CFU assays. Lineage depleted (lin$^-$) cells were harvested from *HRP-2*$^{+/+}$, *HRP-2*$^{+/-}$ and *HRP-2*$^{-/-}$ mice and serially plated. After two rounds of plating, the number of colonies derived from *HRP-2*$^{-/-}$ *and HRP-2*$^{+/-}$ bone marrow cells were respectively 80% and 33% lower compared to the wild-type control (Figure 3B).

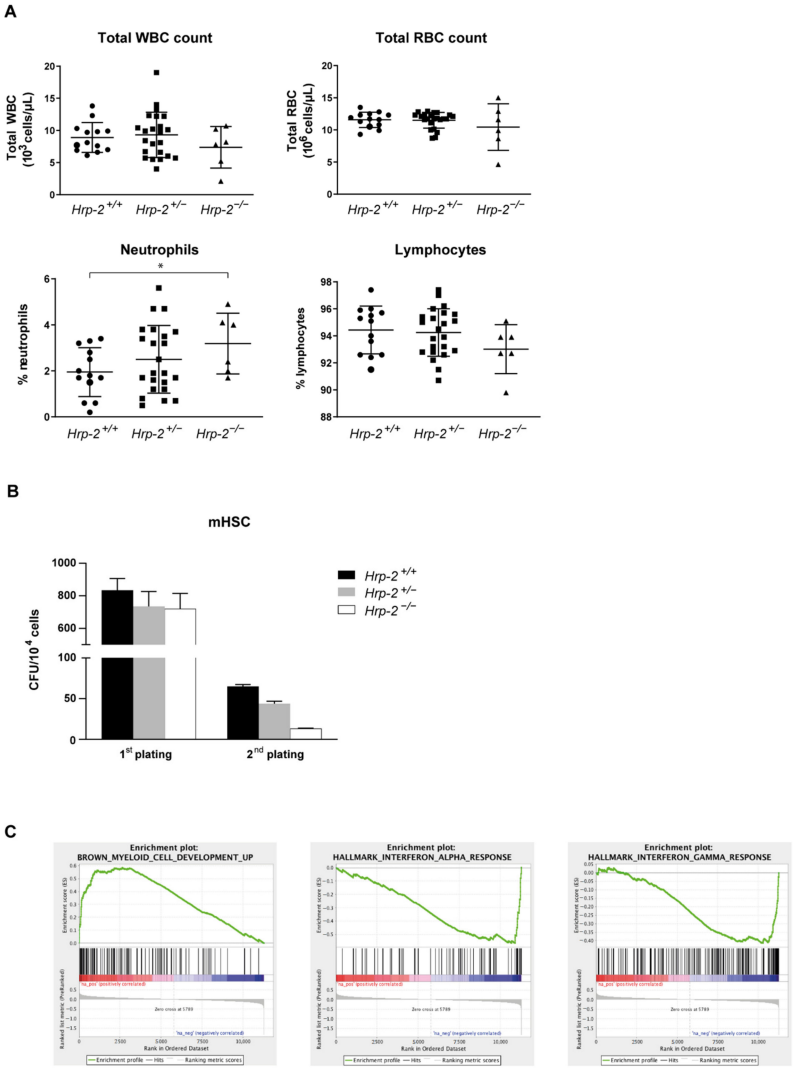

Figure 3. *HRP-2* knockout mice show subtle hematopoietic defects. (**A**) Peripheral blood counts in wild type (*HRP-2*$^{+/+}$), heterozygous (*HRP-2*$^{+/-}$) and knockout (*HRP-2*$^{-/-}$) mice analyzed for total with blood cell (WBC) and total red blood cell (RBC) count (top). Level of neutrophils and lymphocytes (below) are presented as percentage of total differential white blood cell count. Average and standard deviation are indicated. Significance level was determined using two-sided student's *t*-test (* p = 0.042); (**B**) Number of colonies for 10^4 lineage depleted cells harvested from *HRP-2*$^{+/+}$, *HRP-2*$^{+/-}$, and *HRP-2*$^{-/-}$ mice in two consecutive platings in a myeloid CFU assay. Error bars indicate standard deviations of duplicate measurements; (**C**) Gene set enrichment analysis (GSEA) showing a correlation between the RNA profile of *HRP-2*$^{-/-}$ lineage depleted (lin$^-$) bone marrow cells compared to the gene signature of myeloid differentiation and down-regulation of interferon pathways alpha (middle) and gamma (right).

To gain more detailed knowledge of the *HRP-2* knockouts, we performed a gene expression profile analysis, comparing RNA of lin$^-$ bone marrow cells of *HRP-2*$^{+/+}$ and *HRP-2*$^{-/-}$ mice. We found a total of 52 differentially expressed genes (FDR 0.25, Figure S3C), of which 23 were upregulated and 29 were downregulated in *HRP-2*$^{-/-}$ cells. Gene set enrichment analysis (GSEA) uncovered that *HRP-2*$^{-/-}$ cells display a trend towards a gene signature of myeloid differentiation ($p < 2.2 \times 10^{-16}$, Figure 3C). Moreover, the downregulation of interferon alpha and gamma pathways was observed in multiple gene sets ($p < 2.2 \times 10^{-16}$, Figure 3C).

Taken together, these results suggest that HRP-2 depletion reduces the colony formation capacity and induces myeloid differentiation, suggesting that HRP-2 is involved in maintaining the stem-like state of bone marrow cells.

3.4. HRP-2 Depletion Impairs the Clonogenic Growth of Both Human and Mouse Leukemic Cell Lines Independently of MLL Fusions

Next, we investigated the role of HRP-2 in leukemic transformation induced by oncogenic MLL fusions in human leukemic cell lines harboring the MLL-fusions MLL-AF9 (THP1) or MLL-AF4 (SEM), as well as the MLL wild-type leukemic cell lines Kasumi1, K562, and Nalm6. All cell lines were transduced with a lentiviral vector to deplete HRP-2 or with a control vector and plated in methylcellulose. Reduced HRP-2 mRNA and protein levels were verified by qPCR and western blot (Figure S4A–C). Of note, LEDGF/p75 mRNA and protein levels remained unaffected upon HRP-2 depletion (Figure S4A). After 12 days, a decrease in the number of colonies of THP1 (32.8% ± 2.1%) and SEM (51.5% ± 7.0%) cells was observed (Figure 4A, left). Interestingly, the number of colonies in MLL germline cell lines also decreased upon HRP-2 knockdown (Figure 4A, right) with 44.4% ± 27.4% (K562), 38.3% ± 14.2% (Kasumi1) and 19.3% ± 8.8% (Nalm6). Experiments with higher vector titers resulted in an even more pronounced drop in the number of colonies (Figure 4 inserted table), suggesting a concentration-dependent effect. In liquid culture, an impaired cellular growth was observed for SEM and Kasumi1 cells but not for THP1, K562 and Nalm6 cells, excluding that impaired cell growth by HRP-2 depletion is affected in an *MLL*-r-dependent way (Figure S5). Also, for cultured murine lin$^-$ bone marrow cells expressing an MLL-AF9 fusion or a control fusion E2A-HLF, respectively 70% and 56% less colonies were observed after a lentiviral-induced *HRP-2* knockdown (Figure 4B). Taken together, these observations suggest that loss of HRP-2 generally impairs growth of human and murine leukemic cells even in the absence of MLL fusions. To further emphasize that the phenotype observed was independent of MLL, HoxA9 levels were quantified by qPCR (Figure S4D). HoxA9 levels were not significantly affected by HRP-2 depletion.

3.5. HRP-2 Overexpression Rescues MLL-r Clonogenic Growth in LEDGF/p75-Depleted Cells

Since HRP-2 depletion affects the clonogenic growth of all leukemic cell lines tested, we investigated whether HRP-2 overexpression could rescue the colony-forming capacity of an MLL-AF9 leukemic cell line (THP1) after LEDGF/p75 depletion. First, we stably expressed miRNA-resistant LEDGF/p75, HRP-2 or a mock control. Subsequently, cell lines were transduced with a miRNA-based lentiviral vector to specifically knockdown *Psip1* or eGFP (Figure 4C). Expression levels of *Psip1* and *HRP-2* in the generated cell lines were verified by qPCR and western blot (Figure S6A,B). In line with previous reports, LEDGF/p75 depletion caused a ~65% decrease in the number of colonies formed compared to the control [9,12,45] (Figure 4C) and this defect was rescued by LEDGF/p75 back-complementation (BC). Of interest, overexpression of HRP-2 fully restored the CFU activity to wild-type levels, indicating that overexpression of HRP-2 can functionally compensate for the absence of LEDGF/p75 in MLL-transformed cells. This experiment was repeated in the MLL wild-type Nalm6 cell line (Figure S6C–E). In line with published data [12,45], the depletion of LEDGF/p75 did not affect the colony forming capacity of the Nalm6 cell line, as the LEDGF/p75-dependent drop in colonies is MLL-specific. Although both HRP-2 and LEDGF/p75 overexpression increased the colony formation of Nalm6 cells, the effect was not significant.

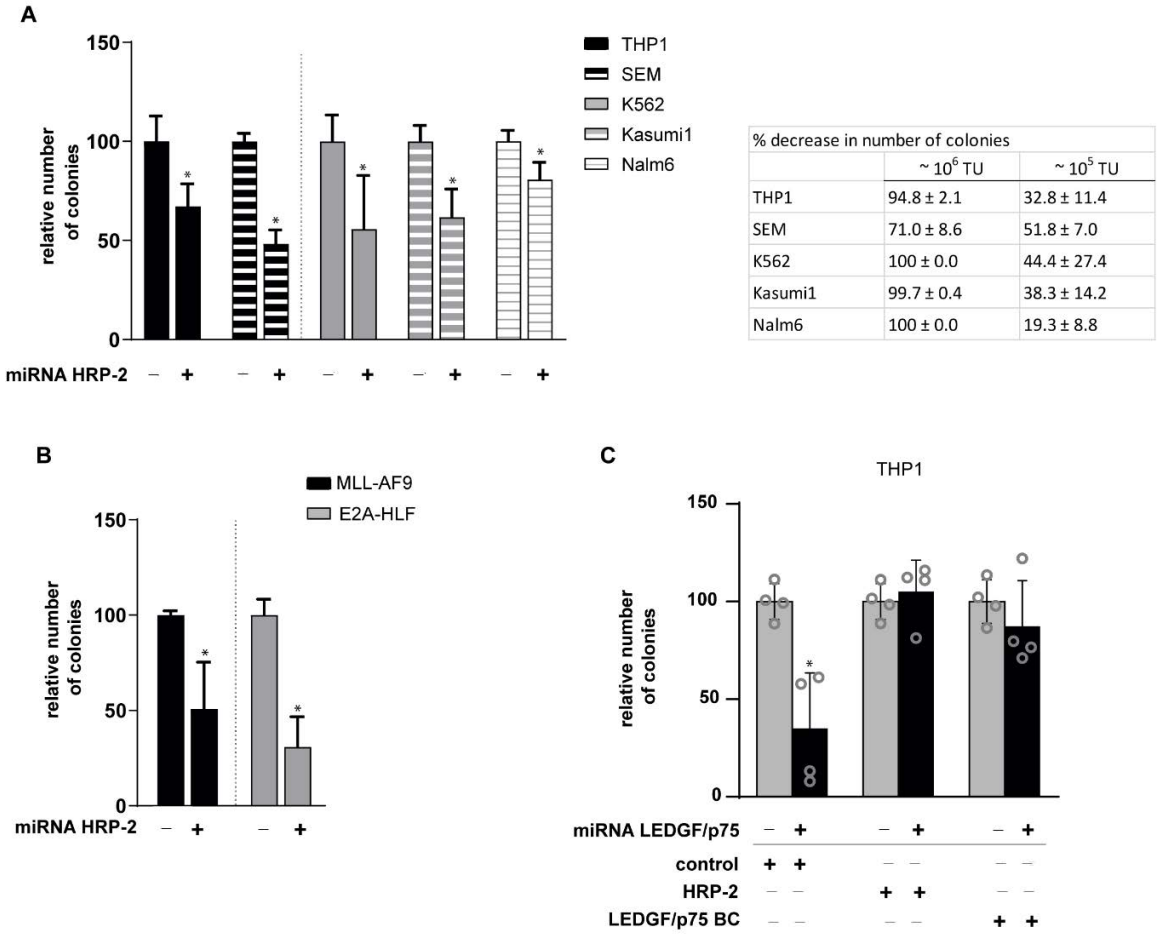

% decrease in number of colonies		
	~ 10^6 TU	~ 10^5 TU
THP1	94.8 ± 2.1	32.8 ± 11.4
SEM	71.0 ± 8.6	51.8 ± 7.0
K562	100 ± 0.0	44.4 ± 27.4
Kasumi1	99.7 ± 0.4	38.3 ± 14.2
Nalm6	100 ± 0.0	19.3 ± 8.8

Figure 4. *HRP-2* knockdown impairs growth in leukemic cell lines, whereas *HRP-2* overexpression rescues the leukemic phenotype. (**A**) Human MLL-transformed cell lines THP1 (MLL-AF9) and SEM (MLL-AF4), as well as wild type MLL cells (Nalm6, Kasumi1, and K562), separated by the dotted line, were transduced with a lentiviral vector encoding a miRNA to knockdown *HRP-2* or a control vector (-). After 12 days in methylcellulose the number of colonies was scored. Counts were normalized to their associated control. Error bars indicate standard deviations of four replicates. Differences were determined using Mann-Whitney U test; * $p < 0.05$. Inserted table describes average percentage decrease in number of colonies for indicated vector titers. TU = titer units (p24 pg/mL) ± S.D.; (**B**) Colony forming assay (CFU) after *HRP-2* knockdown or control (-) of primary bone marrow cells harvested from leukemic mice transplanted with MLL-AF9 or E2A-HLF transduced cells. Counts were normalized to their associated control. Error bars indicate standard deviations of four replicates. Differences were determined using Mann-Whitney U test; * $p < 0.05$; (**C**) Relative number of colonies per 500 plated cells for the THP1 cell line overexpressing miRNA resistant LEDGF/p75, HRP-2 or empty vector (control) after transduction with a lentiviral vector expressing a LEDGF/p75-miRNA to knockdown LEDGF/p75 or a control (black -). Error bars indicate standard deviations of four measurements, individually indicated by a circle. Differences were determined using Mann-Whitney U test; * $p < 0.05$.

3.6. HRP-2 Is Dispensable for the Initiation of MLL-r Leukemia

Our data imply that HRP-2 and LEDGF/p75 own physiological different roles in cells. Therefore, we investigated the involvement of HRP-2 in the initiation of *MLL*-r leukemia. HSC harvested from *HRP-2*$^{+/+}$, *HRP-2*$^{+/-}$ and *HRP-2*$^{-/-}$ mice were transduced with lentiviral vectors encoding one of the most common MLL-fusion proteins (MLL-ENL) or a control fusion inducing ALL (E2A-HLF) and their transformation potentials were compared in serial plating assays (Figure 5A). Remarkably, *HRP-2* wild type, heterozygous, and knockout cells were efficiently transformed by MLL-ENL and E2A-HLF as revealed by the increased number of colonies after three rounds in the CFU assay (Figure 5B). The drop of colonies in the second round in MLL-ENL is likely due to a low transduction

efficiency and represents a selection step prior to transformation. Finally, we performed an in vivo BMT assay. MLL-ENL–expressing *HRP-2*$^{+/+}$, *HRP-2*$^{+/-}$ and *HRP-2*$^{-/-}$ cells were transplanted into lethally irradiated recipient mice and monitored for leukemogenesis. Kaplan-Meier survival plots reveal that mice transplanted with MLL-transformed *HRP-2*$^{+/-}$ and *HRP-2*$^{-/-}$ cells died significantly faster than the transformed wild-type cells (p = 0.02 and p = 0.006, respectively) (Figure 5C), excluding the requirement of HRP-2 in leukemogenesis.

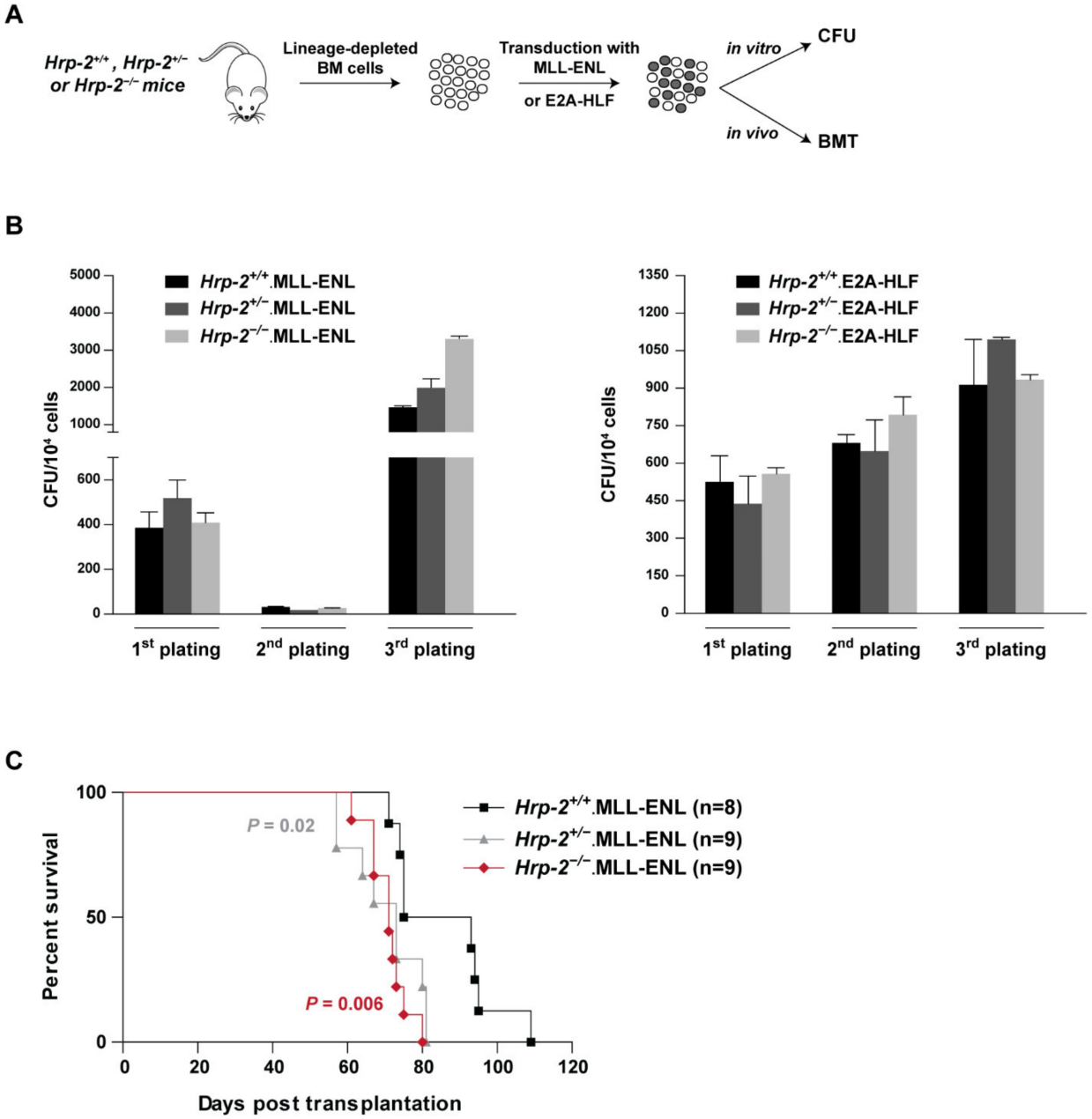

Figure 5. HRP-2 is not required for the initiation of leukemia in vivo. (**A**) Schematic representation of the experimental set up. BM = bone marrow; CFU = colony forming assay; BMT = bone marrow transplantation; (**B**) Colony-forming assay (CFU) for 10^4 *HRP-2*$^{+/+}$, *HRP-2*$^{+/-}$ and *HRP-2*$^{-/-}$ cells transduced with a retroviral vector encoding the MLL-ENL (**B**, left) or E2A-HLF (B, right) fusion. Error bars represent standard deviation of triplicate measurements; (**C**) Kaplan-Meier survival curve from bone marrow transplantation experiments of irradiated mice who received *HRP-2* wild type ($^{+/+}$), heterozygous ($^{+/-}$) or knockout ($^{-/-}$) cells, transduced with mouse stem cell virus (MSCV) MLL-ENL expression vector. Number of transplanted animals (n) per group in indicated. Statistical differences were determined using GraphPad prism.

4. Discussion

Mixed lineage leukemia-rearranged (*MLL*-r) leukemia, a genetically distinct subset of leukemia characterized by *MLL*-rearrangements, is an aggressive form of leukemia without specific treatment options. Currently, many efforts are ongoing to specifically target the oncogenic multi-protein complex involved in *MLL*-r. DOT1L and BET inhibitors target the MLL fusion partners [62,63], whereas menin inhibitors are directly inhibiting MLL binding [64].

The PWWP domain of LEDGF/p75 recognizes H3K36me3 marks associated with active transcription, while the IBD domain binds cellular proteins such as MLL and oncogenic MLL-fusions [46]. MLL fusions are tethered to the chromatin via LEDGF/p75 (encoded by the *Psip1* gene) and interference with this tethering mechanism provides an additional potential target to treat *MLL*-r [12]. Since HRP-2, a paralog of LEDGF/p75 with high sequence similarity, also contains both structured domains and functionally compensates for LEDGF/p75 in the context of HIV [37], we investigated whether HRP-2 is involved in MLL fusion-induced leukemia.

To date, little is known about the function of HRP-2 in cell biology and oncogenesis. Co-immunoprecipitation experiments indicated PogZ, JPO2, and IWS as HRP-2 binding partners [27,31]. We confirmed binding of PogZ and JPO2 to HRP-2 by NMR (Figure S2). In addition, we show for the first time that MLL interacts with the IBD of HRP-2 (Figures 1 and 2 and Figure S2). The role of menin in the MLL-complex has been described before [10] and menin inhibitors induce an MLL specific effect [65]. Whereas menin was required for the stabilization of the MLL-LEDGF/p75 interaction as shown before [9], co-IP experiments with selective MLL-menin interaction inhibitors (Figure 1C,D) and menin-deficient MLL mutants (Figure 1E) revealed that HRP-2 is less dependent on menin. Despite similar binding affinities as measured by NMR and AlphaScreen for the direct binding of HRP-2 or LEDGF/p75 to MLL (Figure 2G,H), co-IP experiments indicate that menin modulates the interaction between the IBD and MLL in favor of LEDGF/p75 (Figure 1). We hypothesize that either low (undetectable) menin levels are sufficient to support this interaction or addition of menin increases the binding affinity of LEDGF/p75 for MLL at the expense of HRP-2. Alternatively, it is possible that the HRP-2-MLL interaction is differentially regulated by PTMs or another cellular factor as compared to the LEDGF/p75-HRP-2 interaction.

We investigated the role of HRP-2 in hematopoiesis in a HRP-2 knockout mouse model. In contrast to Wang et al. [61], the offspring from a heterozygous HRP-2 (HRP-$2^{+/}$) breeding couple deviated from the expected Mendelian inheritance pattern (Table 1), suggesting that HRP-2 is important for postnatal survival. Of note, high postnatal lethality was also observed in systemic Psip1 knockout mice with less than 1% reaching weaning age [66]. Unlike the phenotype observed in Psip1 knockout mice [66], we can only distinguish adult HRP-2 knockout mice from their littermates by small differences in the hematopoietic system compared to wild type and heterozygous littermates (Figure 3). Colony formation experiments (Figure 3B) and Gene Set Enrichment Analysis (Figure 3C) on lin^- HSC hinted towards a stem-like state supported by HRP-2. Recent studies indicated a crucial function of HRP-2 during mRNA transcription [39] and differentiation [67] of muscle cells, suggesting HRP-$2^{-/-}$ muscles fail to support vital functions.

In addition, an analysis of cell survival (Figure 4 and Figure S7) indicates that HRP-2 depletion impairs cellular growth of different types of leukemia, independently of the presence of MLL fusions. Of interest, *HRP-2* knockdown was reported to reduce growth in hepatocellular carcinoma cells and induce cell death in U2OS cells [38], suggesting a more general pro-survival role of HRP-2. Of note, we observed that colony formation of the MLL-driven cell lines THP1 and SEM at high vector titer were less affected by HRP-2 depletion than the MLL wild-type cell lines K562, Kasumi1 and Nalm6 (Figure 4). We hypothesize that HRP-2 and LEDGF/p75 compete for MLL binding, implying that reduced HRP-2 levels facilitate binding between LEDGF/p75, MLL and menin supporting *MLL*-r-induced leukemogenesis.

In fact, while endogenous HRP-2 levels do not rescue colony formation in THP1 cells upon depletion of LEDGF/p75, overexpression of HRP-2 does (Figure 4C). This latter result supports the notion that HRP-2 can function as a tether between the MLL-fusion proteins and its target genes. However, as HRP-2 overexpression also promoted cell growth in hepatocellular carcinoma [31], we cannot exclude that HRP-2 rescues the cellular growth via a more general pathway. This rescue phenotype is reminiscent of that of HRP-2 in HIV infection (25).

Although HRP-2 seems to play an important but nonspecific role in leukemic cell survival, our results indicate that HRP-2 is not important for the initial transformation of hematopoietic stem cells by MLL fusions. MLL-ENL transduced lin$^-$ BMC from *HRP-2* knockout, heterozygous or wild-type mice transformed irrespective of the genotype in a colony forming assay, indicating that *HRP-2* knockdown, nor knockout is impairing MLL-driven leukemogenesis in the presence of LEDGF/p75.

In an in vivo experiment in lethally irradiated mice, engrafted MLL-ENL transduced cells induced MLL leukemia with a survival time of 6 weeks post transplantation (Figure 5C), equal to previously published experiments [12]. Transplantation of MLL-ENL transduced HRP-2$^{-/-}$ or HRP-2$^{+/-}$ cells also resulted in leukemogenesis and the life span of these mice was even shorter. The shorter life span of mice in the absence of HRP-2 may be due to a loss of competition between HRP-2 and LEDGF/p75 for binding to MLL. By competing with LEDGF/p75, HRP-2 could act as a tumor suppressor. Alternatively, although HRP-2 might be dispensable for leukemogenesis, its role in hematopoiesis may affect the survival of mice.

5. Conclusions

In conclusion, our results demonstrate that although HRP-2 interacts with MLL, this interaction is not required for the development of mixed lineage leukemia. LEDGF/p75 is the main driver of *MLL*-r-driven leukemia and menin, a modulator of the relative affinities for MLL, may be responsible for this selectivity by increasing the affinity of MLL for LEDGF/p75. Still, HRP-2 may have a more general role in the survival of leukemic cells independently of MLL.

Supplementary Materials: The following are available online at https://www.mdpi.com/2073-4409/10/1/192/s1, Materials and methods, Figure S1: Assignment of the NMR 2D ^{15}N/^{1}H HSQC spectra of the ^{15}N-labeled HRP-2 IBD, Figure S2: Amino acids perturbed by HRP-2 binding to JPO2 and PogZ are similar to the amino acids perturbed by MLL, Figure S3: validation of HRP-2 mouse model, Figure S4. Validation of HRP-2 knockdown in human and mouse cell lines, Figure S5: HRP-2 depletion variably affects growth of human cell lines, Figure S6: Validation of double transduced THP1 and Nalm6 cells used for CFU experiment, Figure S7: Original blots from co-immunoprecipitation experiments, Figure S8: Original blots to validate HRP-2 and LEDGF/p75 expression levels, Table S1: Statistics for the final water-refined sets of structures.

Author Contributions: S.V.B., S.E.A., J.D.R. and Z.D. designed experiments and wrote the manuscript. S.V.B. and J.D.R. performed co-immunoprecipitation experiments. K.Č. and V.V. generated the NMR data. S.V.B. and S.E.A. performed all cellular and animal experiments. A.C. helped with cellular experiments. F.M., S.G., C.H.H. and P.V.V. analyzed RNA sequencing results. F.C., P.V.V., V.V. and Z.D. supervised the project. All authors have read and agreed to the published version of the manuscript.

Funding: This work was supported by KU Leuven Interdisciplinair onderzoeksprogramma (IDO) Program Grant IDO/12/008-3E130241, Flanders FWO Grant G.0595.13 (Z.D.), the Flemish SBO 140038 (ChromaTarget), the Belgian National Foundation Against Cancer, GACR 16-06357S (V.V.), the Ministry of Education of the Czech Republic LO1304 (V.V.), the European Regional Development Fund; OP RDE; the project ChemBioDrug CZ.02.1.01/0.0/0.0/16_019/0000729 (V.V.), the ERC Starting Grant 639784 (P.V.V.), the Fund for Scientific Research Flanders (FWO) (P.V.V.), Stand up to Cancer (the Flemish cancer society) (P.V.V.), the CPRIT RR170036 grant (H.C.H.), the V Foundation grant V2018-003 (H.C.H.), Gabrielle's Angel Foundation for Cancer Research (H.C.H.) and NCI R00CA187565 (H.C.H.). F.C. is supported by the KU Leuven Industrial Research Fund. S.V.B. has been funded by a fellowship of FWO.

Institutional Review Board Statement: The study was conducted according to the guidelines of the Declaration of Helsinki. All animal experiments were approved by the KU Leuven ethical committee (P201/2014, approved 15th of September 2014).

Informed Consent Statement: Not applicable.

Data Availability Statement: The RNA sequencing dataset generated and analyzed during the current study is available in the NCBI's Gene Expression Omnibus repository (GSE154202). Generated NMR structures are available on the PDB (ID: 6T3I) and BMRB (ID: 34442). Additional data generated in this study is available from the corresponding author Zeger Debyser (Zeger.Debyser@kuleuven.be).

Acknowledgments: We thank Martine Michiels for excellent technical assistance.

Conflicts of Interest: The authors declare no conflict of interest.

References

1. Mohan, M.; Lin, C.; Guest, E.; Shilatifard, A. Licensed to elongate: A molecular mechanism for MLL-based leukaemogenesis. *Nat. Rev. Cancer* **2010**, *10*, 721–728. [CrossRef] [PubMed]
2. Balgobind, B.V.; Hollink, I.H.I.M.; Arentsen-Peters, S.T.C.J.M.; Zimmermann, M.; Harbott, J.; Berna Beverloo, H.; von Bergh, A.R.M.; Cloos, J.; Kaspers, G.J.L.; de Haas, V.; et al. Integrative analysis of type-I and type-II aberrations underscores the genetic heterogeneity of pediatric acute myeloid leukemia. *Haematologica* **2011**, *96*, 1478–1487. [CrossRef] [PubMed]
3. Hilden, J.M.; Dinndorf, P.A.; Meerbaum, S.O.; Sather, H.; Villaluna, D.; Heerema, N.A.; McGlennen, R.; Smith, F.O.; Woods, W.G.; Salzer, W.L.; et al. Analysis of prognostic factors of acute lymphoblastic leukemia in infants: Report on CCG 1953 from the Children's Oncology Group. *Blood* **2006**, *108*, 441–451. [CrossRef] [PubMed]
4. Masetti, R.; Rondelli, R.; Fagioli, F.; Mastronuzzi, A.; Pierani, P.; Togni, M.; Menna, G.; Pigazzi, M.; Putti, M.C.; Basso, G.; et al. Infants with acute myeloid leukemia treated according to the Associazione Italiana di Ematologia e Oncologia Pediatrica 2002/01 protocol have an outcome comparable to that of older children. *Haematologica* **2014**, *99*, e127. [CrossRef] [PubMed]
5. Chessells, J.M.; Harrison, C.J.; Kempski, H.; Webb, D.K. Clinical features, cytogenetics and outcome in acute lymphoblastic and myeloid leukaemia of infancy: Report from the MRC Childhood Leukaemia working party. *Leukemia* **2002**, *12*, 776–784. [CrossRef]
6. Steinhilber, D.; Marschalek, R. How to effectively treat acute leukemia patients bearing MLL-rearrangements? *Biochem. Pharmacol.* **2018**, *147*, 183–190. [CrossRef]
7. Meyer, C.; Schneider, B.; Jakob, S.; Strehl, S.; Attarbaschi, A.; Schnittger, S.; Schoch, C.; Jansen, M.W.J.C.; van Dongen, J.J.M.; den Boer, M.L.; et al. The MLL recombinome of acute leukemias. *Leuk. Off. J. Leuk. Soc. Am. Leuk. Res. Fund UK* **2006**, *20*, 777–784. [CrossRef]
8. Slany, R.K. The molecular mechanics of mixed lineage leukemia. *Oncogene* **2016**, *35*, 5215–5223. [CrossRef]
9. Yokoyama, A.; Cleary, M.L. Menin Critically Links MLL Proteins with LEDGF on Cancer-Associated Target Genes. *Cancer Cell* **2008**, *14*, 36–46. [CrossRef]
10. Yokoyama, A.; Somervaille, T.C.P.; Smith, K.S.; Rozenblatt-Rosen, O.; Meyerson, M.; Cleary, M.L. The menin tumor suppressor protein is an essential oncogenic cofactor for MLL-associated leukemogenesis. *Cell* **2005**, *123*, 207–218. [CrossRef]
11. Caslini, C.; Yang, Z.; El-Osta, M.; Milne, T.A.; Slany, R.K.; Hess, J.L. Interaction of MLL Amino Terminal Sequences with Menin Is Required for Transformation. *Cancer Res.* **2007**, *67*, 7275–7283. [CrossRef]
12. El Ashkar, S.; Schwaller, J.; Pieters, T.; Goossens, S.; Demeulemeester, J.; Christ, F.; Van Belle, S.; Juge, S.; Boeckx, N.; Engelman, A.; et al. LEDGF/p75 is dispensable for hematopoiesis but essential for MLL-rearranged leukemogenesis. *Blood* **2018**, *131*, 95–107. [CrossRef]
13. Dietz, F.; Franken, S.; Yoshida, K.; Nakamura, H.; Kappler, J.; Gieselmann, V. The family of hepatoma-derived growth factor proteins: Characterization of a new member HRP-4 and classification of its subfamilies. *Biochem. J.* **2002**, *366*, 491–500. [CrossRef] [PubMed]
14. El-Tahir, H.; Dietz, F.; Dringen, R.; Schwabe, K.; Strenge, K.; Kelm, S.; Abouzied, M.; Gieselmann, V.; Franken, S. Expression of hepatoma-derived growth factor family members in the adult central nervous system. *BMC Neurosci.* **2006**, *7*, 6. [CrossRef]
15. Izumoto, Y.; Kuroda, T.; Harada, H.; Kishimoto, T.; Nakamura, H. Hepatoma-derived growth factor belongs to a gene family in mice showing significant homology in the amino terminus. *Biochem. Biophys. Res. Commun.* **1997**, *238*, 26–32. [CrossRef] [PubMed]
16. Wu, H.; Zeng, H.; Lam, R.; Tempel, W.; Amaya, M.F.; Xu, C.; Dombrovski, L.; Qiu, W.; Wang, Y.; Min, J. Structural and histone binding ability characterizations of human PWWP domains. *PLoS ONE* **2011**, *6*, e18919. [CrossRef] [PubMed]
17. Daugaard, M.; Baude, A.; Fugger, K.; Povlsen, L.K.; Beck, H.; Sørensen, C.S.; Petersen, N.H.T.; Sorensen, P.H.B.; Lukas, C.; Bartek, J.; et al. LEDGF (p75) promotes DNA-end resection and homologous recombination. *Nat. Struct. Mol. Biol.* **2012**, *19*, 803–810. [CrossRef] [PubMed]
18. Daugaard, M.; Kirkegaard-Sørensen, T.; Ostenfeld, M.S.; Aaboe, M.; Høyer-Hansen, M.; Ørntoft, T.F.; Rohde, M.; Jäättelä, M. Lens epithelium-derived growth factor is an Hsp70-2 regulated guardian of lysosomal stability in human cancer. *Cancer Res.* **2007**, *67*, 2559–2567. [CrossRef]

19. Wu, X.; Daniels, T.; Molinaro, C.; Lilly, M.B.; Casiano, C.A. Caspase cleavage of the nuclear autoantigen LEDGF/p75 abrogates its pro-survival function: Implications for autoimmunity in atopic disorders. *Cell Death Differ.* **2002**, *9*, 915–925. [CrossRef]
20. Singh, D.P.; Ohguro, N.; Chylack, L.T.; Shinohara, T. Lens epithelium-derived growth factor: Increased resistance to thermal and oxidative stresses. *Investig. Ophthalmol. Vis. Sci.* **1999**, *40*, 1444–1451.
21. Basu, A.; Drame, A.; Muñoz, R.; Gijsbers, R.; Debyser, Z.; De Leon, M.; Casiano, C.A. Pathway specific gene expression profiling reveals oxidative stress genes potentially regulated by transcription co-activator LEDGF/p75 in prostate cancer cells. *Prostate* **2012**, *72*, 597–611. [CrossRef] [PubMed]
22. Basu, A.; Rojas, H.; Banerjee, H.; Cabrera, I.B.; Perez, K.Y.; de León, M.; Casiano, C.A. Expression of the stress response oncoprotein LEDGF/p75 in human cancer: A study of 21 tumor types. *PLoS ONE* **2012**, *7*. [CrossRef] [PubMed]
23. Sapoznik, S.; Cohen, B.; Tzuman, Y.; Meir, G.; Ben-Dor, S.; Harmelin, A.; Neeman, M. Gonadotropin-regulated lymphangiogenesis in ovarian cancer is mediated by LEDGF-induced expression of VEGF-C. *Cancer Res.* **2009**, *69*, 9306–9314. [CrossRef] [PubMed]
24. Huang, T.S.; Myklebust, L.M.; Kjarland, E.; Gjertsen, B.T.; Pendino, F.; Bruserud, Ø.; Døskeland, S.O.; Lillehaug, J.R. LEDGF/p75 has increased expression in blasts from chemotherapy-resistant human acute myelogenic leukemia patients and protects leukemia cells from apoptosis in vitro. *Mol. Cancer* **2007**, *6*, 31. [CrossRef]
25. Singh, D.K.; Gholamalamdari, O.; Jadaliha, M.; Li, X.L.; Lin, Y.C.; Zhang, Y.; Guang, S.; Hashemikhabir, S.; Tiwari, S.; Zhu, Y.J.; et al. PSIP1/p75 promotes tumorigenicity in breast cancer cells by promoting the transcription of cell cycle genes. *Carcinogenesis* **2017**, *38*, 966–975. [CrossRef]
26. Maertens, G.N.; Cherepanov, P.; Engelman, A. Transcriptional co-activator p75 binds and tethers the Myc-interacting protein JPO2 to chromatin. *J. Cell Sci.* **2006**, *119*, 2563–2571. [CrossRef]
27. Bartholomeeusen, K.; Christ, F.; Hendrix, J.; Rain, J.-C.; Emiliani, S.; Benarous, R.; Debyser, Z.; Gijsbers, R.; De Rijck, J. Lens epithelium-derived growth factor/p75 interacts with the transposase-derived DDE domain of PogZ. *J. Biol. Chem.* **2009**, *284*, 11467–11477. [CrossRef]
28. Hughes, S.; Jenkins, V.; Dar, M.J.; Engelman, A.; Cherepanov, P. Transcriptional co-activator LEDGF interacts with Cdc7-activator of S-phase kinase (ASK) and stimulates its enzymatic activity. *J. Biol. Chem.* **2010**, *285*, 541–554. [CrossRef]
29. Tesina, P.; Čermáková, K.; Hořejší, M.; Procházková, K.; Fábry, M.; Sharma, S.; Christ, F.; Demeulemeester, J.; Debyser, Z.; De Rijck, J.; et al. Multiple cellular proteins interact with LEDGF/p75 through a conserved unstructured consensus motif. *Nat. Commun.* **2015**, *6*, 7968. [CrossRef]
30. Sharma, S.; Čermáková, K.; De Rijck, J.; Demeulemeester, J.; Fábry, M.; El Ashkar, S.; Van Belle, S.; Lepšík, M.; Tesina, P.; Duchoslav, V.; et al. Affinity switching of the LEDGF/p75 IBD interactome is governed by kinase-dependent phosphorylation. *Proc. Natl. Acad. Sci. USA* **2018**, *115*, E7053–E7062. [CrossRef]
31. Gao, K.; Xu, C.; Jin, X.; Wumaier, R.; Ma, J.; Peng, J.; Wang, Y.; Tang, Y.; Yu, L.; Zhang, P. HDGF-related protein-2 (HRP-2) acts as an oncogene to promote cell growth in hepatocellular carcinoma. *Biochem. Biophys. Res. Commun.* **2015**, *458*, 849–855. [CrossRef] [PubMed]
32. Cherepanov, P.; Maertens, G.; Proost, P.; Devreese, B.; Van Beeumen, J.; Engelborghs, Y.; De Clercq, E.; Debyser, Z. HIV-1 integrase forms stable tetramers and associates with LEDGF/p75 protein in human cells. *J. Biol. Chem.* **2003**, *278*, 372–381. [CrossRef] [PubMed]
33. Cherepanov, P.; Devroe, E.; Silver, P.A.; Engelman, A. Identification of an evolutionarily conserved domain in human lens epithelium-derived growth factor/transcriptional co-activator p75 (LEDGF/p75) that binds HIV-1 integrase. *J. Biol. Chem.* **2004**, *279*, 48883–48892. [CrossRef] [PubMed]
34. Ciuffi, A.; Llano, M.; Poeschla, E.; Hoffmann, C.; Leipzig, J.; Shinn, P.; Ecker, J.R.; Bushman, F. A role for LEDGF/p75 in targeting HIV DNA integration. *Nat. Med.* **2005**, *11*, 1287–1289. [CrossRef] [PubMed]
35. Llano, M.; Saenz, D.T.; Meehan, A.; Wongthida, P.; Peretz, M.; Walker, W.H.; Teo, W.; Poeschla, E.M. An Essential Role for LEDGF/p75 in HIV Integration. *Science (80-.)* **2006**, *314*, 461–464. [CrossRef]
36. Shun, M.C.; Raghavendra, N.K.; Vandegraaff, N.; Daigle, J.E.; Hughes, S.; Kellam, P.; Cherepanov, P.; Engelman, A. LEDGF/p75 functions downstream from preintegration complex formation to effect gene-specific HIV-1 integration. *Genes Dev.* **2007**, *21*, 1767–1778. [CrossRef] [PubMed]
37. Schrijvers, R.; De Rijck, J.; Demeulemeester, J.; Adachi, N.; Vets, S.; Ronen, K.; Christ, F.; Bushman, F.D.; Debyser, Z.; Gijsbers, R. LEDGF/p75-independent HIV-1 replication demonstrates a role for HRP-2 and remains sensitive to inhibition by LEDGINs. *PLoS Pathog.* **2012**, *8*. [CrossRef]
38. Baude, A.; Aaes, T.L.; Zhai, B.; Al-Nakouzi, N.; Oo, H.Z.; Daugaard, M.; Rohde, M.; Jäättelä, M. Hepatoma-derived growth factor-related protein 2 promotes DNA repair by homologous recombination. *Nucleic Acids Res.* **2016**, *44*, 2214–2226. [CrossRef]
39. LeRoy, G.; Oksuz, O.; Descostes, N.; Aoi, Y.; Ganai, R.A.; Kara, H.O.; Yu, J.-R.; Lee, C.-H.; Stafford, J.; Shilatifard, A.; et al. LEDGF and HDGF2 relieve the nucleosome-induced barrier to transcription in differentiated cells. *Sci. Adv.* **2019**, *5*, eaay3068. [CrossRef]
40. Zhang, X.; Chen, Y.; Pan, J.; Liu, X.; Chen, H.; Zhou, X.; Yuan, Z.; Wang, X.; Mo, D. iTRAQ-based quantitative proteomic analysis reveals the distinct early embryo myofiber type characteristics involved in landrace and miniature pig. *BMC Genomics* **2016**, *17*, 137. [CrossRef]
41. Hu, Y.; He, C.; Liu, J.P.; Li, N.S.; Peng, C.; Yang-Ou, Y.B.; Yang, X.Y.; Lu, N.H.; Zhu, Y. Analysis of key genes and signaling pathways involved in Helicobacter pylori-associated gastric cancer based on The Cancer Genome Atlas database and RNA sequencing data. *Helicobacter* **2018**, *23*. [CrossRef] [PubMed]

42. Geraerts, M.; Michiels, M.; Baekelandt, V.; Debyser, Z.; Gijsbers, R. Upscaling of lentiviral vector production by tangential flow filtration. *J. Gene Med.* **2005**, *7*, 1299–1310. [CrossRef] [PubMed]
43. Maertens, G.; Cherepanov, P.; Pluymers, W.; Busschots, K.; De Clercq, E.; Debyser, Z.; Engelborghs, Y. LEDGF/p75 is essential for nuclear and chromosomal targeting of HIV-1 integrase in human cells. *J. Biol. Chem.* **2003**, *278*, 33528–33539. [CrossRef] [PubMed]
44. De Rijck, J.; Vandekerckhove, L.; Gijsbers, R.; Hombrouck, A.; Hendrix, J.; Vercammen, J.; Engelborghs, Y.; Christ, F.; Debyser, Z. Overexpression of the lens epithelium-derived growth factor/p75 integrase binding domain inhibits human immunodeficiency virus replication. *J. Virol.* **2006**, *80*, 11498–11509. [CrossRef]
45. Méreau, H.; De Rijck, J.; Čermáková, K.; Kutz, A.; Juge, S.; Demeulemeester, J.; Gijsbers, R.; Christ, F.; Debyser, Z.; Schwaller, J. Impairing MLL-fusion gene-mediated transformation by dissecting critical interactions with the lens epithelium-derived growth factor (LEDGF/p75). *Leukemia* **2013**, *27*, 1245–1253. [CrossRef]
46. Cermakova, K.; Tesina, P.; Demeulemeester, J.; El Ashkar, S.; Méreau, H.; Schwaller, J.; \vRezáčová, P.; Veverka, V.; De Rijck, J. Validation and structural characterization of the LEDGF/p75-MLL interface as a new target for the treatment of MLL-dependent leukemia. *Cancer Res.* **2014**, *74*, 5139–5151. [CrossRef]
47. Renshaw, P.S.; Veverka, V.; Kelly, G.; Frenkiel, T.A.; Williamson, R.A.; Gordon, S.V.; Hewinson, R.G.; Carr, M.D. Sequence-specific assignment and secondary structure determination of the 195-residue complex formed by the Mycobacterium tuberculosis proteins CFP-10 and ESAT-6. *J. Biomol. NMR* **2004**, *30*, 225–226. [CrossRef]
48. Veverka, V.; Lennie, G.; Crabbe, T.; Bird, I.; Taylor, R.J.; Carr, M.D. NMR assignment of the mTOR domain responsible for rapamycin binding. *J. Biomol. NMR* **2006**, *36* (Suppl. 1), 3. [CrossRef]
49. Herrmann, T.; Güntert, P.; Wüthrich, K. Protein NMR structure determination with automated NOE assignment using the new software CANDID and the torsion angle dynamics algorithm DYANA. *J. Mol. Biol.* **2002**, *319*, 209–227. [CrossRef]
50. Shen, Y.; Delaglio, F.; Cornilescu, G.; Bax, A. TALOS+: A hybrid method for predicting protein backbone torsion angles from NMR chemical shifts. *J. Biomol. NMR* **2009**, *44*, 213–223. [CrossRef]
51. Harjes, E.; Harjes, S.; Wohlgemuth, S.; Müller, K.-H.; Krieger, E.; Herrmann, C.; Bayer, P. GTP-Ras Disrupts the Intramolecular Complex of C1 and RA Domains of Nore1. *Structure* **2006**, *14*, 881–888. [CrossRef] [PubMed]
52. Yokogawa, M.; Kobashigawa, Y.; Yoshida, N.; Ogura, K.; Harada, K.; Inagaki, F. NMR Analyses of the Interaction between the FYVE Domain of Early Endosome Antigen 1 (EEA1) and Phosphoinositide Embedded in a Lipid Bilayer. *J. Biol. Chem.* **2012**, *287*, 34936–34945. [CrossRef] [PubMed]
53. NorCOMM2-Phenotyping-Project. Available online: http://www.norcomm2.org/norcomm2/index.php (accessed on 18 January 2020).
54. Moll, P.; Ante, M.; Seitz, A.; Reda, T. QuantSeq 3′ mRNA sequencing for RNA quantification. *Nat. Methods* **2014**, *11*, i–iii. [CrossRef]
55. Dobin, A.; Davis, C.A.; Schlesinger, F.; Drenkow, J.; Zaleski, C.; Jha, S.; Batut, P.; Chaisson, M.; Gingeras, T.R. STAR: Ultrafast universal RNA-seq aligner. *Bioinformatics* **2013**, *29*, 15–21. [CrossRef]
56. Love, M.I.; Huber, W.; Anders, S. Moderated estimation of fold change and dispersion for RNA-seq data with DESeq2. *Genome Biol.* **2014**, *15*, 550. [CrossRef]
57. Grembecka, J.; He, S.; Shi, A.; Purohit, T.; Muntean, A.G.; Sorenson, R.J.; Showalter, H.D.; Murai, M.J.; Belcher, A.M.; Hartley, T.; et al. Menin-MLL inhibitors reverse oncogenic activity of MLL fusion proteins in leukemia. *Nat. Chem. Biol.* **2012**, *8*, 277–284. [CrossRef]
58. Borkin, D.; Pollock, J.; Kempinska, K.; Purohit, T.; Li, X.; Wen, B.; Zhao, T.; Miao, H.; Shukla, S.; He, M.; et al. Property Focused Structure-Based Optimization of Small Molecule Inhibitors of the Protein-Protein Interaction between Menin and Mixed Lineage Leukemia (MLL). *J. Med. Chem.* **2016**, *59*, 892–913. [CrossRef]
59. Huang, J.; Gurung, B.; Wan, B.; Matkar, S.; Veniaminova, N.A.; Wan, K.; Merchant, J.L.; Hua, X.; Lei, M. The same pocket in menin binds both MLL and JUND but has opposite effects on transcription. *Nature* **2012**, *482*, 542–546. [CrossRef]
60. Blokken, J.; De Rijck, J.; Christ, F.; Debyser, Z. Protein–protein and protein–chromatin interactions of LEDGF/p75 as novel drug targets. *Drug Discov. Today Technol.* **2017**, *24*, 25–31. [CrossRef]
61. Wang, H.; Shun, M.-C.; Dickson, A.K.; Engelman, A.N. Embryonic Lethality Due to Arrested Cardiac Development in Psip1/Hdgfrp2 Double-Deficient Mice. *PLoS ONE* **2015**, *10*, e0137797. [CrossRef]
62. Daigle, S.R.; Olhava, E.J.; Therkelsen, C.A.; Majer, C.R.; Sneeringer, C.J.; Song, J.; Johnston, L.D.; Scott, M.P.; Smith, J.J.; Xiao, Y.; et al. Selective killing of mixed lineage leukemia cells by a potent small-molecule DOT1L inhibitor. *Cancer Cell* **2011**, *20*, 53–65. [CrossRef]
63. Dawson, M.A.; Prinjha, R.K.; Dittmann, A.; Giotopoulos, G.; Bantscheff, M.; Chan, W.-I.; Robson, S.C.; Chung, C.; Hopf, C.; Savitski, M.M.; et al. Inhibition of BET recruitment to chromatin as an effective treatment for MLL-fusion leukaemia. *Nature* **2011**, *478*, 529–533. [CrossRef]
64. Borkin, D.; He, S.; Miao, H.; Kempinska, K.; Pollock, J.; Chase, J.; Purohit, T.; Malik, B.; Zhao, T.; Wang, J.; et al. Pharmacologic Inhibition of the Menin-MLL Interaction Blocks Progression of MLL Leukemia In~Vivo. *Cancer Cell* **2015**, *27*, 589–602. [CrossRef]
65. Aguilar, A.; Zheng, K.; Xu, T.; Xu, S.; Huang, L.; Fernandez-Salas, E.; Liu, L.; Bernard, D.; Harvey, K.P.; Foster, C.; et al. Structure-Based Discovery of M-89 as a Highly Potent Inhibitor of the Menin-Mixed Lineage Leukemia (Menin-MLL) Protein–Protein Interaction. *J. Med. Chem.* **2019**, *62*, 6015–6034. [CrossRef]

66. Sutherland, H.G.; Newton, K.; Brownstein, D.G.; Holmes, M.C.; Kress, C.; Semple, C.A.; Bickmore, W.A. Disruption of Ledgf/Psip1 results in perinatal mortality and homeotic skeletal transformations. *Mol. Cell. Biol.* **2006**, *26*, 7201–7210. [CrossRef]
67. Zhu, X.; Lan, B.; Yi, X.; He, C.; Dang, L.; Zhou, X.; Lu, Y.; Sun, Y.; Liu, Z.; Bai, X.; et al. HRP2-DPF3a-BAF complex coordinates histone modification and chromatin remodeling to regulate myogenic gene transcription. *Nucleic Acids Res.* **2020**, *48*, 6563–6582. [CrossRef]